1584

RESEARCH ARTICLE

Statistical parametric mapping of the regional distribution and ontogenetic scaling of foot pressures during walking in Asian elephants (*Elephas maximus*)

Olga Panagiotopoulou[1],*, Todd C. Pataky[2], Zoe Hill[1] and John R. Hutchinson[1]

[1]Structure and Motion Laboratory, Department of Veterinary Basic Sciences, The Royal Veterinary College, University of London, Hatfield, AL9 7TA, UK and [2]Department of Bioengineering, Shinshu University, Ueda 386-8567, Japan

*Author for correspondence (opanagiotopoulou@rvc.ac.uk)

SUMMARY

Foot pressure distributions during locomotion have causal links with the anatomical and structural configurations of the foot tissues and the mechanics of locomotion. Elephant feet have five toes bound in a flexible pad of fibrous tissue (digital cushion). Does this specialized foot design control peak foot pressures in such giant animals? And how does body size, such as during ontogenetic growth, influence foot pressures? We addressed these questions by studying foot pressure distributions in elephant feet and their correlation with body mass and centre of pressure trajectories, using statistical parametric mapping (SPM), a neuro-imaging technology. Our results show a positive correlation between body mass and peak pressures, with the highest pressures dominated by the distal ends of the lateral toes (digits 3, 4 and 5). We also demonstrate that pressure reduction in the elephant digital cushion is a complex interaction of its viscoelastic tissue structure and its centre of pressure trajectories, because there is a tendency to avoid rear 'heel' contact as an elephant grows. Using SPM, we present a complete map of pressure distributions in elephant feet during ontogeny by performing statistical analysis at the pixel level across the entire plantar/palmar surface. We hope that our study will build confidence in the potential clinical and scaling applications of mammalian foot pressures, given our findings in support of a link between regional peak pressures and pathogenesis in elephant feet.

Supplementary material available online at http://jeb.biologists.org/cgi/content/full/215/9/1584/DC1

Key words: plantar pressure, locomotion, elephant, statistical parametric mapping, random field theory.

INTRODUCTION

Elephant feet (manus and pes) are fascinating structures because they combine very stiff and compliant tissues roughly distributed between the cranial and caudal portions of the foot, respectively (Fig. 1). Thus, the mechanics of the foot should exhibit marked regional variations across a stance phase. Cranially, the five digits (as well as nails and sole/slipper) form a hoof-like structure around the perimeter of the feet. Caudally and centrally, a highly compliant fibrous–fatty pad (comprising multiple connected cushions) dominates the foot area (Weissengruber et al., 2006). Furthermore, the orientations of the bones of elephant feet are highly unusual, again hinting at complex mechanical functions. The skeletal posture is best termed subunguligrade because only the tips of the phalanges (*via* their nails) are in approximate contact with the substrate. Yet the functional posture is more plantigrade, especially in the more horizontally oriented pes, because the massive foot pad and associated structures (e.g. prepollex and prehallux or 'predigits') connect the proximal carpal/tarsal bones with the substrate. These structures should direct some unknown portion of the ground reaction force (GRF) directly proximally rather than through the distal phalanges, as in truly plantigrade animals (D'Aout et al., 2010; Michilsens et al., 2009; Miller et al., 2008).

Bizarre structural mechanics aside, elephant feet are interesting because they face extreme biomechanical constraints in order to support the weight of the largest land animal. Michilsens et al. presented a broad comparative dataset for mammalian foot pressures and found that elephant feet closely fit the general trend of isometric scaling, so their peak foot pressures should not be relatively greater than those of other animals (Michilsens et al., 2009). Surely the enlarged foot pad of elephants helps to distribute the pressures across the foot and keep peak pressures low, but how? Are excessively high foot pressures, which may cause damage to the sole's soft tissues, mitigated more passively by the viscoelastic pad in the caudal and central parts of the elephant foot, or are they mitigated behaviourally, by more active control of regional foot loading patterns? Do foot pressure trajectories change with size, potentially to adapt to the scaling of pressures during growth, or do elephants maintain the same spatiotemporal mechanics across ontogeny? These questions are interesting from a pure scaling perspective – to understand one extreme example of how large animals support their weight on their feet will improve understanding of how foot support changes with size. Miller et al. showed that different components of the forefeet and hindfeet scale at different ontogenetic rates in elephants (Miller et al., 2008). The forefoot bones and tendons generally follow isometry or negative allometry (becoming more slender) whereas the hindfoot bones and tendons tend to exhibit more positive allometry (becoming more robust). Regions of the feet also grow at different rates. The metapodial bones of the forefeet (manus) tend to grow the fastest laterally (digits 4 and 5), whereas those of the hindfeet (pes) grow fastest medially (digit 1) and laterally (digits 4 and 5). Based on these findings, Miller et al. (Miller et al., 2008) proposed that this scaling may indicate regional loading on the feet and thereby differences in regional mechanics within and between feet as well as across ontogeny.

Fig. 1. Sagittal plane cross-section of an elephant left pes. Cranially, the foot consists of five very stiff digits (as well as nails and sole/slipper), which form a hoof-like structure around the perimeter of the foot. Caudally and centrally, a highly compliant and viscoelastic fat pad dominates the foot area. For more information on elephant foot anatomy see Weissengruber et al. (Weissengruber et al., 2006).

Furthermore, elephant foot pressure mechanics have fundamental importance for the welfare of captive elephants worldwide. An accurate characterization of normal foot pressures in elephants should be pivotal for predicting and monitoring foot pathologies such as trauma, osteomyelitis, osteoarthritis and ankylosis of the joints (Fowler and Mikota, 2006). Such pathologies are blamed for causing 50% of mortalities in captive elephants (Csuti et al., 2001). A thorough description of foot pressures in elephants and their relationship with pathogenesis could also benefit the planning of

sole/nail trimming and substrate choice for elephant enclosures (Fowler and Mikota, 2006).

In this study we aimed to test four hypotheses by recording the pressure distributions on Asian elephant (*Elephas maximus* Linnaeus 1758) feet during walking. Our study sample included an ontogenetic growth series of elephants to assess ontogenetic changes of foot dynamics using statistical parametric mapping (SPM). Hypothesis 1 addresses Miller et al.'s suggestion that the ontogenetic scaling of foot structures is correlated with pressure differences (Miller et al., 2008). If this is correct, the highest pressures should occur on digits 4–5 in the manus and digits 1 and 4–5 in the pes, and these pressure differences should become more pronounced with increasing body mass.

Hypothesis 2 poses that peak pressures in the manus and pes are maintained at a roughly constant level with increasing size, at dynamically similar speeds (normal walking; Froude number Fr ~0.10 for $Fr=v^2/gl$, where v is speed, g is acceleration due to gravity and l is hip height). This not only is an expectation of dynamic similarity theory (Alexander and Jayes, 1983) but also is expected if material properties, especially strength, of foot sole tissues remain roughly the same across ontogeny (maintaining sufficient safety factors to avoid injury to the sensitive foot sole), although the scaling of pressures will be influenced by the differential growth of foot subregions (Miller et al., 2008).

Similar to the human heel fat pad, the elephant foot fat pad presumably functions as a shock absorber when the foot hits the ground, as a result of its viscoelastic properties. Thus, it is expected to reduce plantar/palmar pressures. Nevertheless, foot pressure reductions can also be achieved *via* increasing the surface area that the pressure is applied to, because pressure (P) equals force (**F**) per surface area (A). We thus propose hypothesis 3: reduction of pressure on the caudal and central aspect of the elephant foot fat pad is not solely due to its viscoelastic nature but is likely to result from a complex and dynamic interaction of behavioural preferences, as manifested in centre of pressure (COP) trajectories and viscoelastic material properties.

Finally, *via* hypothesis 4 we sought to determine whether the regional incidence of foot pathologies in elephants corresponds with high regional foot pressures. Anecdotal accounts from our discussions with elephant keepers and from our post-mortem

Table 1. Subject characteristics (species: *Elephas maximus*) and number of experimental trials

	Subject 1	Subject 2	Subject 3	Subject 4	Subject 5	Subject 6
Age	31 days	1 year	3 years	14 years	16 years	27 years
Sex	M	F	M	F	F	F
Body mass (kg)	120	500	1042	2820	2920	3332
Contact area (cm²)						
Manus	198	334	559	902	933	949
Pes	157	300	485	752	805	688
Mean mid-stance pressure (N cm⁻²)						
Fore left	2.1	5.8	5.1	7.4		
Fore right	2.1	5.6	5.5		9.6	7.0
Hind left	1.6	4.7	4.5	8.2	6.9	
Hind right	1.8	3.9	4.6	8.1	7.7	6.5
Total mid-stance force (% body weight)						
Fore left	24.9	30.9	23.1	22.9		
Fore right	24.3	29.7	25.8		30.0	16.9
Hind left	14.1	20.6	17.9	18.0	17.4	
Hind right	15.5	17.3	17.3	19.0	17.4	9.3
Location	Whipsnade	Whipsnade	Whipsnade	Woburn	Woburn	Whipsnade
Number of trials	104	43	33	28	32	104

Contact areas were measured from peak plantar pressure records thresholded at 0.05 N cm⁻².
Subjects 6 and 1 are mother and child and participated together.

database on elephant cadaveric feet at The Royal Veterinary College suggest that digits 3, 4 and 5 of the manus and pes are most susceptible to pathology, particularly degenerative joint disease (Csuti et al., 2001; Fowler and Mikota, 2006). If there is a relationship between pathologies and foot pressures, the highest pressures should occur in digits 3, 4 and 5 of the manus and pes, and the lowest pressures in digits 1 and 2. Our aim was not to determine whether these pathologies truly do statistically predominate in digits 3, 4 and 5, which will be examined in another study, but to test whether there is an association between these anecdotal accounts and rigorously quantified pressure patterns. If the hypothesis is upheld, this will build confidence in the potential clinical applications of elephant foot pressure analysis.

MATERIALS AND METHODS
Design

Six Asian elephants from two zoological parks in Bedfordshire, UK (the Zoological Society of London's Whipsnade Zoo and Woburn Safari Park) were selected to participate in this study. They ranged in age and body mass from 31 days and 120 kg to 27 years and 3332 kg (Table 1), thus spanning an almost 28-fold range of body masses. Keepers gave clinically informed consent and the study was approved by The Royal Veterinary College's Ethics Committee.

A 5 m walkway was constructed on top of flat concrete with sufficient space for an elephant to turn at each end. A thin foam pad 3 m long and 0.4 m wide was laid on top of the concrete at the start of the walkway and was followed by a 1.0×0.4 m pressure plate equipped with 8192 sensors (Footscan; RSscan, Olen, Belgium) and a final 1 m length of foam pad. A thin black rubber covering was placed on top of the whole walkway to avoid recognition of the plate location by the elephants and their keepers. A Sony HDR (Sony, London, UK) high definition video camera was used to record walking speed. The camera faced perpendicular to the walkway and was placed 5 m from the COP plate. Sampling frequencies of the camera and pressure plate were set at 25 and 250 Hz, respectively.

Prior to each data collection session, the pressure plate was calibrated with a person of known mass measured on a digital scale (±0.1 kg), as per the manufacturer's instructions. The elephants were guided over the walkway at an overall mean steady speed of $1.0 \, \text{m s}^{-1}$ (mean Fr 0.10) by park keepers, an average of 50 times each (see Table 1). Unsteady trials with apparent acceleration and deceleration were excluded. The experimental techniques used did not involve or cause any discomfort to the elephants.

Data pre-processing

All subsequently described analyses were implemented in Python 2.7 using NumPy 1.5.1, SciPy 0.9 and Matplotlib 1.0 (Enthought Python Distribution version 7.0; Enthought Inc., Austin, TX, USA). The raw $(x, y,$ time) pressure plate data were exported from the Footscan system for custom analysis. Single footsteps, i.e. stance phases, from each trial were isolated algorithmically using spatiotemporal gaps between clusters of non-zero pressure voxels (see supplementary material Movie 1). Henceforth, individual footsteps are referred to as 'images' [note that these are 3D spatiotemporal images with two spatial and one temporal dimension(s)]. As the elephants' feet were large with respect to the size of the measurement plate and because data acquisition (with a limited buffer size) could not always be triggered appropriately, many images were spatially and/or temporally incomplete. Individual images were thus manually assessed for spatiotemporal completeness according to four inclusion criteria (see Fig. 2 and Table 2). Images were discarded if they failed to meet either full-spatial and half-temporal completeness or full-temporal and half-
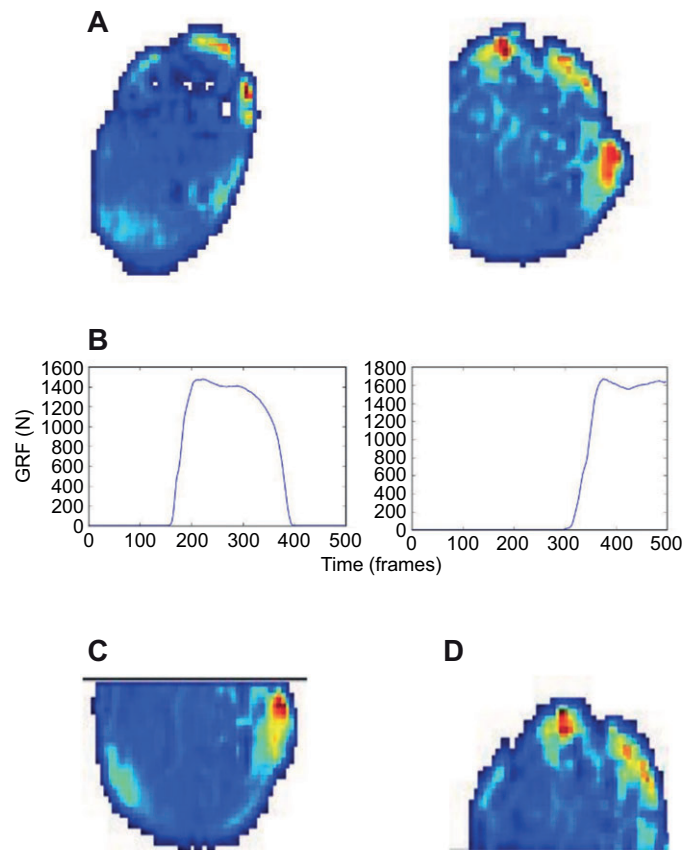

Fig. 2. Example image inclusion criteria. (A) Spatially complete pes (left), spatially incomplete manus (right). (B) Temporally complete ground reaction force (GRF) *vs* time data from the pressure pad (left), temporally incomplete GRF *vs* time data (right). (C) Rear contact of manus. (D) Fore contact of manus.

spatial completeness (all criteria were judged qualitatively). The remaining footsteps were manually identified as left/right and manus/pes.

All images were spatially scaled in the direction of progression by a factor of 1.5, using bilinear interpolation to compensate for the non-square measurement grid of the RSscan system (7.62×5.08 mm, manufacturer specified). To promote efficient and high-resolution homologous data comparison, the scaled images were spatially registered (Maintz and Viergever, 1998) within-subjects and within-feet (Fig. 3). Registration aimed to re-align the footsteps, which landed on the pressure plate in arbitrary postures, by transforming each footstep image into a standard homologous

Table 2. Image inclusion criteria (see also Fig. 2)

Criterion	Description	Notes
A	Spatially complete	Entire plantar surface visible
B	Temporally complete	Entire GRF trajectory intact; GRF had to start and end at 0 N
C	Rear contact	Most posterior contact point visible
D	Fore contact	Most anterior contact point visible

GRF, ground reaction force (foot area × foot pressure) extrapolated from pressure pad data.
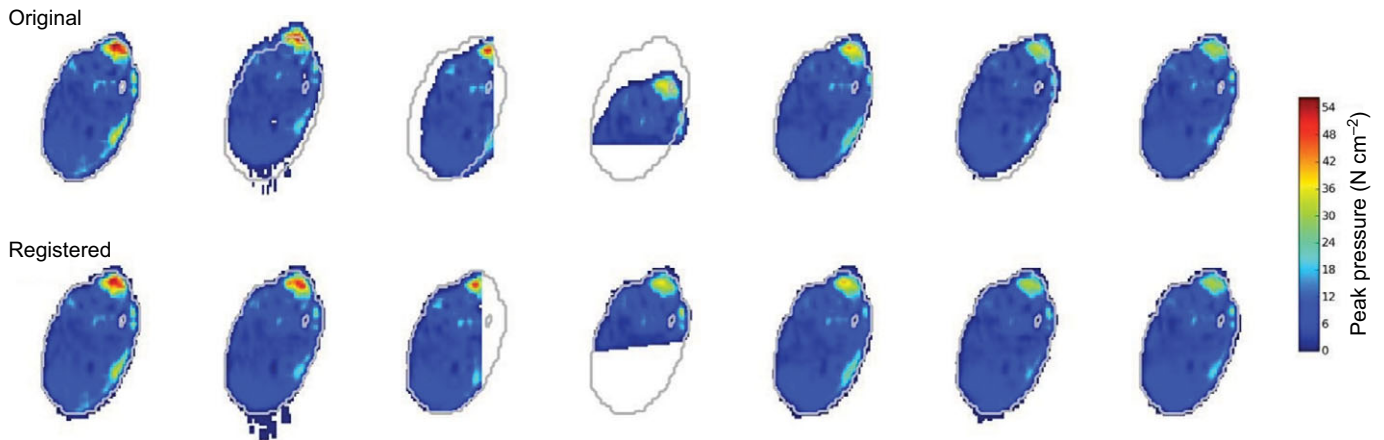Images that did not meet either A and 50% of B, or B and 50% of A were discarded.

Fig. 3. Example image registration for a subset of subject 3's right pes steps. The grey outline indicates the orientation of the template image to which the others were registered. Stray marks behind the heel in the second sample in particular are low-pressure records from skidding/skimming of the foot before heel strike.

space. We found that existing pedobarographic registration algorithms (e.g. Pataky et al., 2008; Oliveira et al., 2010) failed to perform consistently well on the elephant data, probably because these algorithms were developed for human feet, whose highly asymmetric shapes offer valuable registration-relevant information. Rather than develop a new elephant-specific registration algorithm, we opted to register the images manually using a graphical-user interface, an approach that has been shown to perform as well as optimal algorithmic registration in humans (Pataky et al., 2008). The template foot image was presented as an isocontour (threshold $0.05\,\mathrm{N\,cm^{-2}}$), and the source image was manually translated and rotated. The template image selected for each subject and each foot was the chronologically first step that met both the A and B spatiotemporal completion criteria (see above).

Between-subjects registration was computed by adding a symmetric spatial scaling transformation (dx, dy, $d\theta$, ds where s is scale). The template foot image selected for the between-subjects registration was the largest and chronologically first step that met both the A and B spatiotemporal completion criteria. Similar to the within-subject registration, qualitative optimal alignment across subjects was conducted manually.

Following scaling and registration, all images were reduced to 2D summary peak pressure (i.e. spatially maximal pressure over the entire stance phase) images and seven homologous anatomical regions of interest (ROI) were manually digitized (Fig. 4). ROIs 1–5 respectively represent digits 1–5. ROI 6 is located in the middle of the plantar/palmar foot surface whereas ROI 7 is located on the caudal-most aspect of the sole (Fig. 4). Peak pressures ($\mathrm{N\,cm^{-2}}$) were extracted from a 3-pixel neighbourhood surrounding each digitized ROI using a weighted Gaussian kernel mean window with a standard deviation of one pixel. SPM for hypotheses 1, 2 and 4 was used to conduct statistical analyses at the pixel level, thereby describing broad pressure distribution changes across the entire surface of the sole. ROI procedures were subsequently used to explicitly test the parts of the hypotheses that pertained to specific foot regions. Finally, COP trajectories were used to infer behavioural foot-loading preferences.

Statistical analysis
SPM
SPM is a digital imaging technique that is effective for analysing smooth or piecewise-smooth dimensional field processes. Where

a single experimental observation is a lattice sample (e.g. foot pressure distribution, measured over a spatial lattice), multiple observations can, in general, be aligned such that homologous structures overlap optimally. After such alignment, SPM conducts statistical tests at each pixel (i.e. at each lattice node) in a mass-univariate manner (Friston et al., 2007). The result is an SPM, or a statistical parametric map, which is a lattice sampling of the underlying statistical field. That is, just as each pixel (or lattice node) originally contained a single value of the measured variable (e.g. pressure), pixels in an SPM contain a single statistical value (usually t- or F-values). SPM has previously been used in
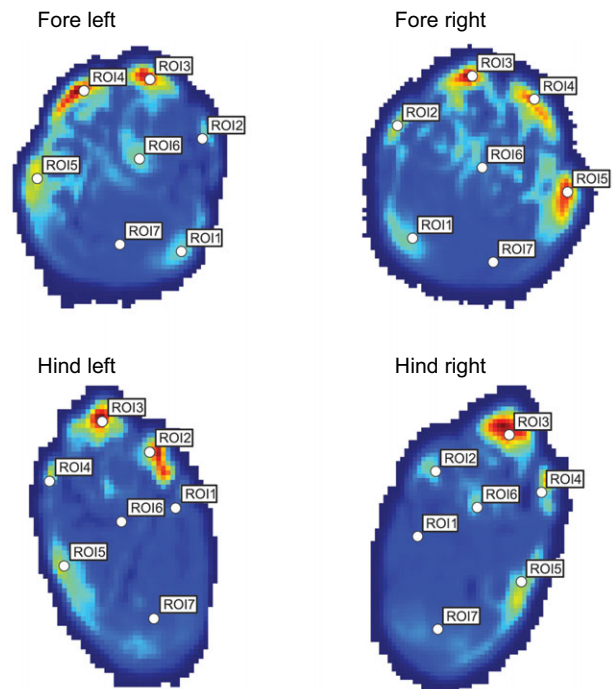

Fig. 4. Regions of interest (ROI) representing anatomical structures from registered images of elephant manus (fore left and right) and pedes (hind left and right). ROIs 1–5 represent the five elephant foot digits. ROIs 6 and 7 represent the middle and caudal-most aspects of the foot, respectively. Note the slight toeing-in of the manus and toeing-out of the pes.
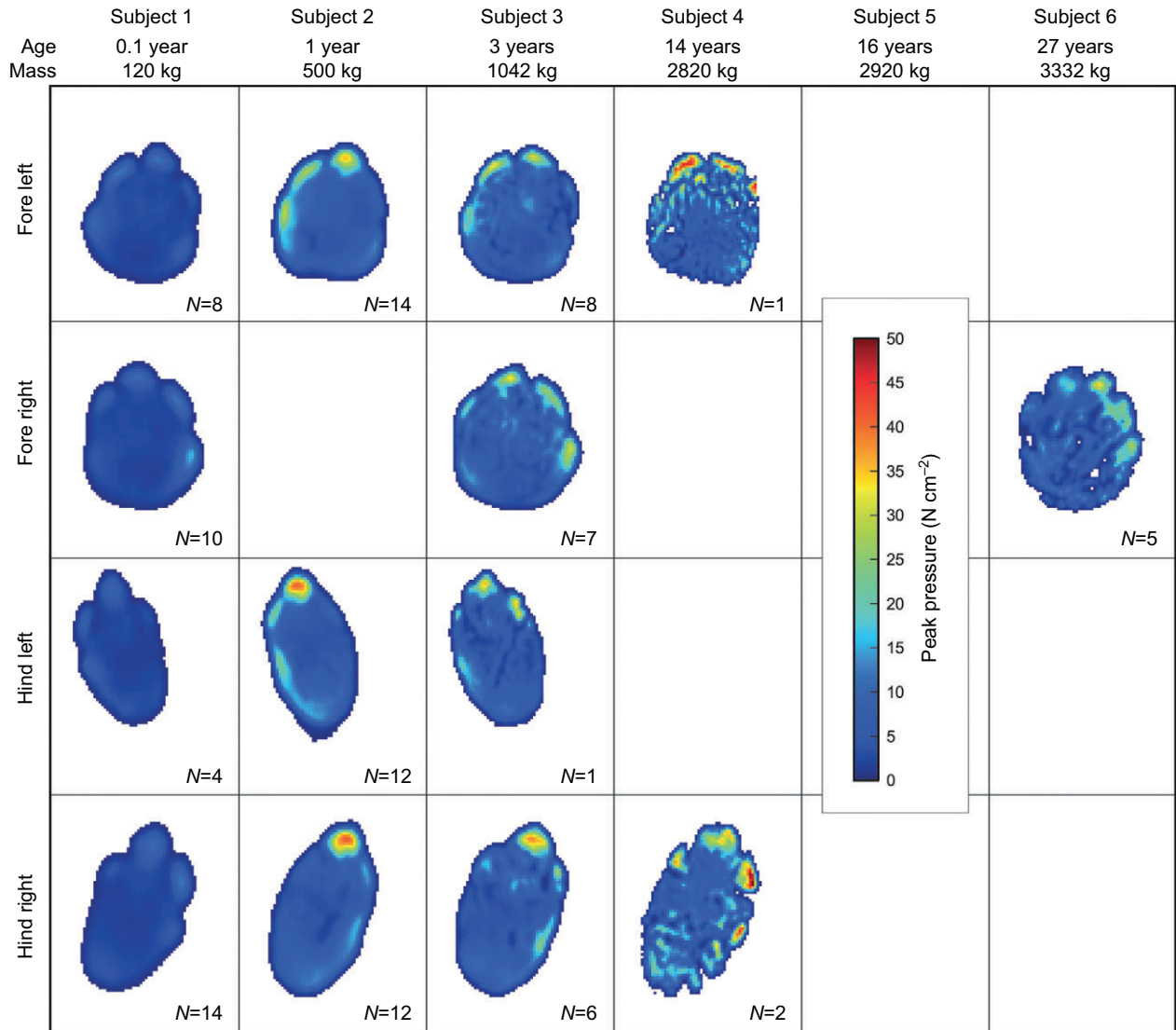
Fig. 5. Mean peak pressure images for each subject and each foot. The number of observations (N) meeting the 'spatial and temporal completeness' criteria is indicated for each foot. Missing data are due to the lack of a large sample size, which is required to produce the mean peak pressure images. Nevertheless, peak pressure values were exported for all individuals and used for the statistical analysis.

neuroimaging (Friston et al., 2007) and human foot studies (Pataky, 2008; Pataky and Goulermas, 2008; Pataky et al., 2008) but it has never been used for animal studies and in particular never for the study of the foot pressure distribution of elephants or across ontogeny in mammals.

Here, we used linear regression between ontogenetic factors (body mass) and pressure, so the present SPMs contain t-values that represent the ratio between the regression slope and the variance about that regression line. The significance of the SPM was assessed using random field theory, which computes and assigns P-values to supra-threshold clusters (i.e. pixel clusters that survived a t threshold) based on their spatial extent. The clusters that exceeded the critical cluster size provided evidence of non-random processes induced by experimental manipulation. Subsequent ROI analyses, which probed specific areas of the SPM based on the present anatomically specific hypotheses, were conducted using linear mixed models (SPSS 1.8, IBM Corporation, Armonk, NY, USA). Statistical significance was set at $P=0.05$.

COP

We computed the resultant contact point, or COP, at foot strike by initially computing the mean peak pressure image for each foot across subjects and by thresholding these images at $0.5\,\mathrm{N\,cm^{-2}}$. We then manually digitized the cranial-most and caudal-most points along the foot's longitudinal axis and computed the whole COP trajectory as the pressure-weighted image centroid. Lastly, we resolved the COP location at time=0 (i.e. initial foot contact) into the percentage distance between the cranial- and caudal-most foot points.

RESULTS
SPM

The distribution of the mean peak pressure for each subject and each foot is shown in Fig. 5. The youngest and smallest elephant (subject 1) has significantly lower mean whole-foot peak pressure values than all other elephants ($P<0.05$; Table 1). Subjects 2 and 3, who were close in age and body mass, display significantly different ($P<0.05$) pressure values to subjects 1 and 6. Specifically, the pressure values of subjects 2 and 3 are higher than those of subject
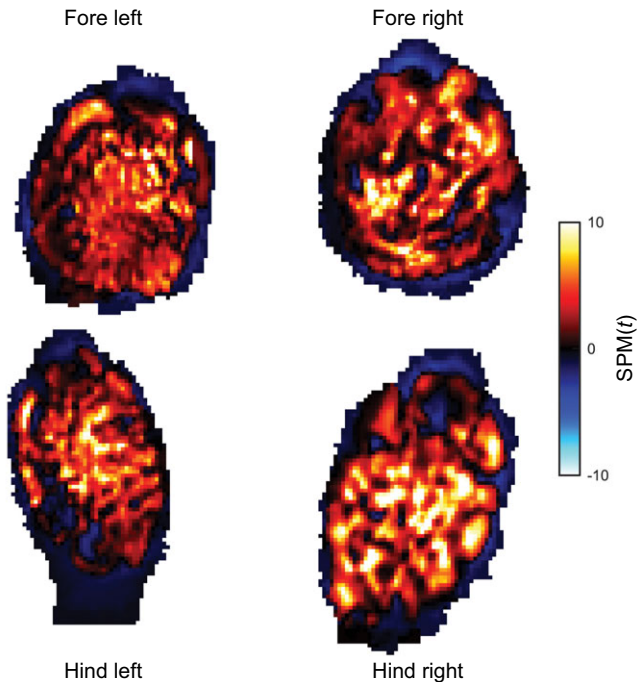
Fore left   Fore right

Hind left   Hind right

SPM(*t*)

Fig. 6. The raw statistical parametric mapping (SPM)(*t*) results using random field theory. SPM(*t*) values represent the ratio between the regression slope and the variance about that regression line. Warm colours (red/yellow) display a positive correlation between body mass and pressure; cold colours (blue/black) show a negative correlation.

1, and lower than those of subject 6 (Table 1). Subjects 4 and 5 exhibit significant differences in pressure values from those of the smallest elephants (higher than values for subjects 1, 2 and 3).
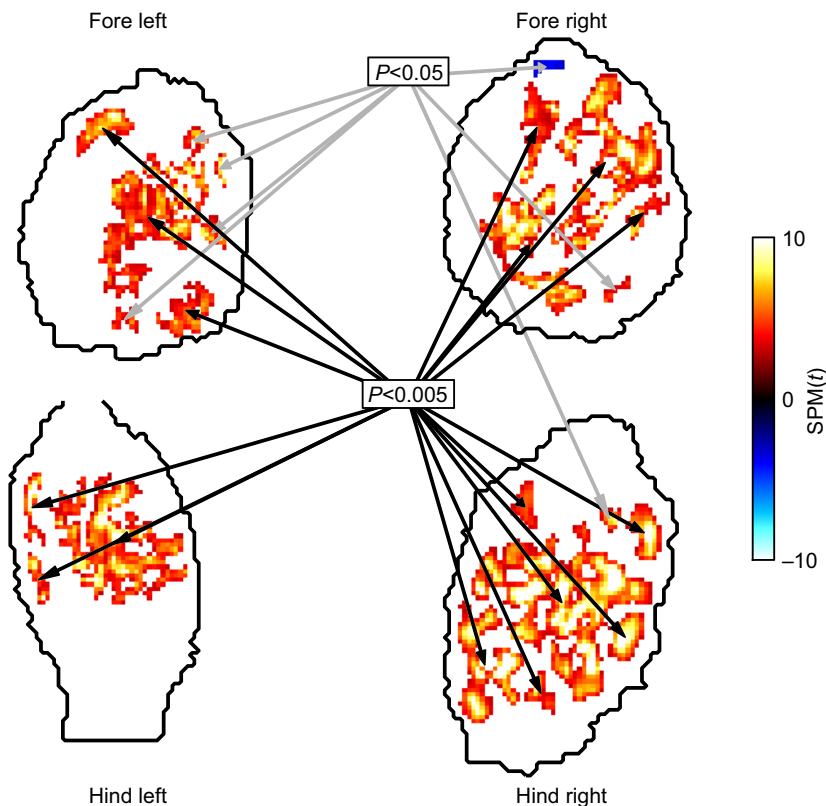
Ideally, for a comparative ontogenetic analysis of pressure distributions, a larger sample size would be needed for subjects 4, 5 and 6. Constraints due to the large size of the feet of adult elephants coupled with the small size of the pressure pad prevented us from collecting more data for the adult elephants. Nevertheless, this limitation should not have an effect on our general results because pressures across the whole foot have a statistically significant positive correlation with body mass (i.e. they increase with body mass) (Figs 6, 7), but pressure increases are not limited to a particular area, spanning broadly over most of each foot's surface (Figs 6, 7).

Specifically, ROIs 3, 4 and 5 for the manus and pes exhibit significantly higher pressure values ($P<0.05$) than all other ROIs (Fig. 8). In contrast, the medial aspects of the manus (Fig. 8A) and pes (Fig. 8B) (i.e. ROI 1 and 2) have the lowest pressure values, which are not significantly different in magnitude ($P>0.9$) from those of ROIs 6 and 7, located at the middle and caudal-most part of the foot, respectively; this finding (Fig. 8) is also reflected in the SPM results (Figs 6, 7). However, limiting analysis to specific points neglects neighbouring regions, which may reach significance. Thus, contrary to SPM, which provides a complete reflection of plantar/palmar pressure distributions across the entire foot, ROI analysis can be biased if used independently and not as a supplement to SPM results.

SPM whole-foot peak pressure magnitudes are, on average, not significantly different ($P>0.05$) between feet. While the pressure histograms have highly positive skewness (i.e. many low-pressure values, fewer mid-range values, and even fewer high-pressure values), the mean metric is presently used because of its physical as opposed to its statistical meaning. That is, this metric represents the ratio of the instantaneous vertical GRF to the instantaneous contact area, and this physical concept is independent of the underlying distribution. In general, the right feet show higher
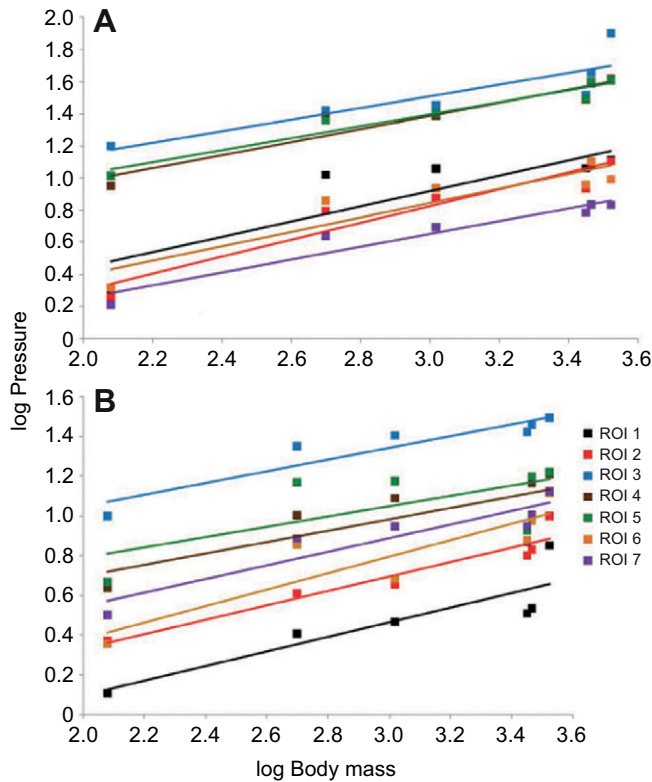

Fore left   Fore right

P<0.05

P<0.005

Hind left   Hind right

SPM(*t*)

Fig. 7. SPM(*t*) with cluster-specific *P*-values. Here *P*-values indicate the probability with which a supra-threshold cluster (|*t*|>3.0) of a given size could have occurred by chance, given the foot size and the pressure field smoothness. Clusters with *P*>0.05 have been removed.

Fig. 8. Linear regressions (with r^2 values) for log pressures (N cm^{-2}) of all ROIs against log body mass (kg) for elephant manus (A) and pes (B). All regressions were significant at $P<0.05$. (A) Manus: ROI 1, $y=0.4763x–0.5098$, $r^2=0.75$; ROI 2, $y=0.5248x–0.7504$, $r^2=0.91$; ROI 3, $y=0.359x+0.431$, $r^2=0.75$; ROI 4, $y=0.3877x+0.1552$, $r^2=0.82$; ROI 5, $y=0.3742x+0.2741$, $r^2=0.94$; ROI 6, $y=0.4485x–0.5023$, $r^2=0.84$; ROI 7, $y=0.3983x–0.5452$, $r^2=0.92$. (B) Pes: ROI 1, $y=0.3675x–0.638$, $r^2=0.77$; ROI 2, $y=0.3629x–0.3927$, $r^2=0.91$; ROI 3, $y=0.2961x+0.4546$, $r^2=0.87$; ROI 4, $y=0.2863x+0.1247$, $r^2=0.58$; ROI 5, $y=0.2585x+0.2735$, $r^2=0.45$; ROI 6, $y=0.4131x–0.4449$, $r^2=0.79$; ROI 7, $y=0.3442x–0.1446$, $r^2=0.86$.

is greater for the manus than for the pedes of all subjects; but note that these values do not generally add up to 100% of body weight (26–78% total for percentage force data in Table 1; except for subject 2, 98.5%) because of incomplete and variable data, so generalizations are difficult to establish. The statistical analysis from ROI (zone-based) data agrees with the SPM analysis in that mean regional peak pressure values are significantly higher ($P<0.05$) for the manus than the pes. However, in contrast to the forefoot *vs* hindfoot pressure difference of 5% found in the SPM analysis, our ROI analysis finds an average difference of 73% (mean ± s.e.m.: manus 18±13 N cm^{-2}, pes 10.4±6.7 N cm^{-2}), which is largely explained by higher mean pressures in the manual digits, especially ROIs 3–5 (Fig. 8).

The SPM and the supplementary ROI results of our study partially support hypothesis 1 because although there is a positive correlation between body mass and pressure magnitudes, the highest pressures are encountered in ROIs (digits) 3 and 5 and to a lesser degree 4, and the lowest pressures are displayed in ROIs 1, 2, 6 and 7. These results also agree with hypothesis 4: greater peak pressures in ROIs 3–5 correspond with supposedly greater foot pathologies in digits 3–5 for the manus and the pes. Hypothesis 2 is rejected because peak pressures increase with body mass.

COP

Fig. 9 shows COP trajectories for each subject and each foot. COP locations at initial foot contact, relative to foot length, are displayed in Fig. 10. Aside from the youngest elephant (subject 1), there appears to be an increasing tendency to avoid rear 'heel' contact as an elephant grows. Instead, a more anterior initial contact point in growing elephants (Fig. 9) implies that the foot is closer to horizontal at initial contact, and thus that contact pressures are dissipated over a larger area during very early stance. This may represent a protective adaptation to avoid high focal tissue stresses. Subject 1 displays COP trajectories different from those of the rest of the subjects, probably as a result of its somewhat awkward gait (visually apparent during experiments, and attributed to its young age). Overall, our results are consistent with hypothesis 3.

DISCUSSION

Foot pressure distributions in elephants were examined in a previous study using traditional statistical approaches of a very limited data set (2 individuals, 3 footsteps) as part of a comparative analysis of mammalian foot pressures (Michilsens et al., 2009). Whilst that study advanced our understanding of peak pressure distribution in

mean peak pressure magnitudes (by about 10%) than the left feet but this difference is not significant ($P>0.05$) and there is considerable intraspecific variation (Table 3). The manus exhibit significantly higher ($P<0.05$) mean peak pressure magnitudes that the pedes (by about 5%) for all subjects (Table 3). Also, as expected the total mid-stance force as a percentage of body weight

Table 3. Pairwise comparisons of mean peak pressure between feet

Foot	Mean peak pressure (±s.e.m.) (N cm^{-2})	Pairwise comparisons	Mean difference between feet (±s.e.m.)	Significance[†]
Fore left	6.2±0.15	Fore right	−0.065±0.161	1.000
		Hind left	0.689±0.175*	0.001
		Hind right	0.867±0.153*	0.000
Fore right	6.3±0.12	Fore left	0.065±0.161	1.000
		Hind left	0.755±0.165*	0.000
		Hind right	0.932±0.141*	0.000
Hind left	5.5±0.14	Fore left	−0.689±0.175*	0.001
		Fore right	−0.755±0.165*	0.000
		Hind right	0.178±0.157	1.000
Hind right	5.4±0.11	Fore left	−0.867±0.153*	0.000
		Fore right	−0.932±0.141*	0.000
		Hind left	−0.178±0.157	1.000

*Mean difference significant at the 0.05 level.
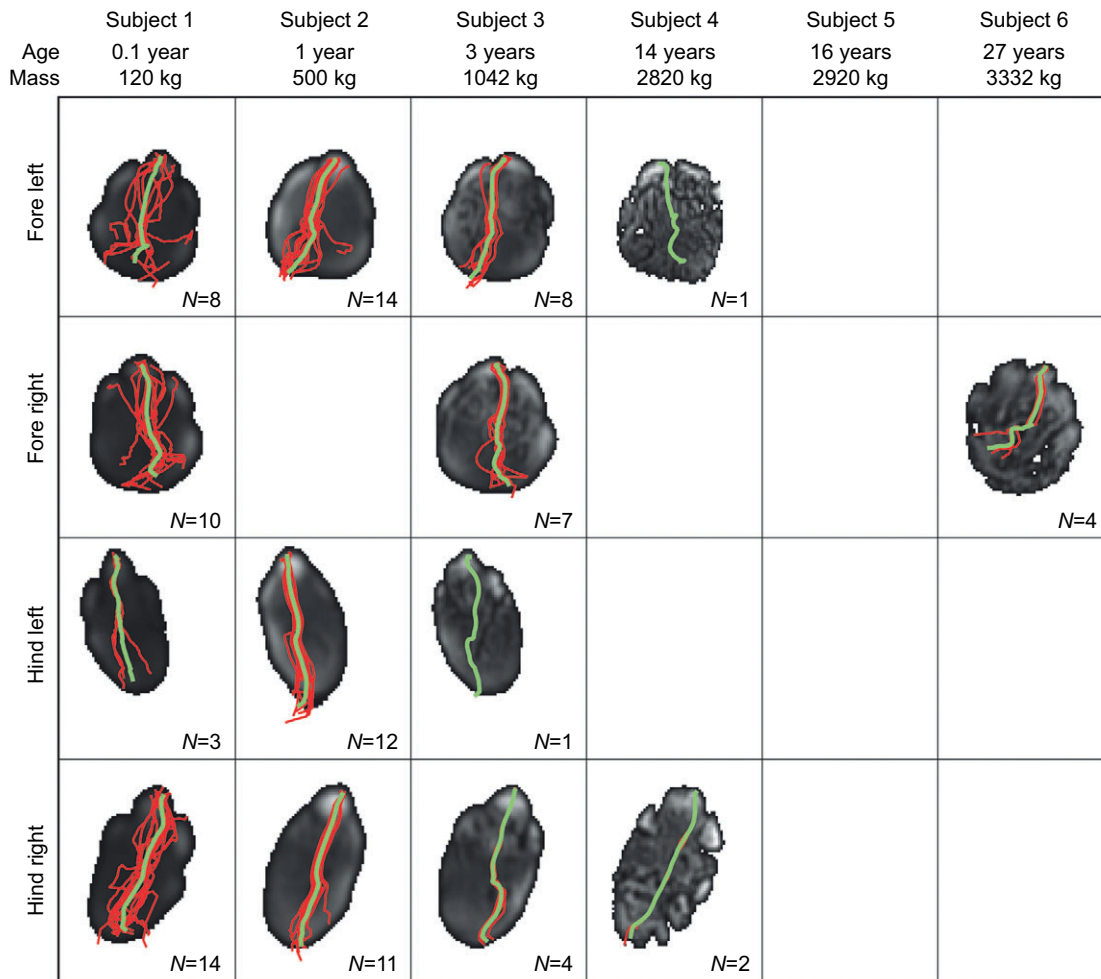[†]Adjustment for multiple comparisons was conducted using Bonferroni corrections.

Fig. 9. Centre of pressure (COP) trajectories for each subject and each foot. Red lines indicate COPs from individual steps, and green lines indicate the mean COP trajectory. The number of observations meeting the spatial and temporal completeness criteria (*N*) is indicated for each foot. Missing data are due to the lack of a large sample size, which is required to produce the average peak pressure images. Nevertheless, peak pressure values were exported for all individuals and used for the statistical analysis.

mammalian feet during walking, such approaches have their limitations. Characterization of foot pressure distribution was conducted over discrete zones, assuming that these are functionally independent, and thus overlooking intra-zone variability. Such a limitation could be vital for studies with clinical, or very specific, applications, such as when the link between pathogenesis or other biomechanical factors and peak pressure distribution is assessed.

Here, we studied the distribution and scaling of foot sole pressures and their possible links to pathologies in walking elephants using SPM. In contrast to traditional statistical approaches, SPM allows one to conduct statistical tests at the same spatial resolution as the original dataset, thereby avoiding the assumption that anatomical regions within elephant feet are functionally independent. Instead, SPM takes into account the statistical correlation amongst neighbouring pixels and summarizes complex pressure field changes as a field-wide statistical map, thereby maintaining anatomical objectivity. This objectivity is a crucial element for thoroughly understanding the mechanical variation of elephant feet during ontogeny and to examine the almost unstudied potential link between foot pressures and pathogenesis in large mammals. Furthermore, a pixel-level statistical analysis for the quantification of plantar/palmar pressure distributions in elephants, as the largest

living land mammals, is essential for a more complete understanding of the correlation between ontogenetic scaling of foot structures and regional pressure variations. It could even aid predictions of how the feet of large extinct animals (e.g. sauropod dinosaurs) may have functioned or how elephant foot mechanics evolved, and thus could test how well the general principles formulated for extant clades apply to other lineages (Alexander et al., 1986); how reliably can foot function be reconstructed from form?

Miller et al. quantified the shape changes in elephant feet with increasing body mass, showing that different components of the manus and pes scale at different ontogenetic rates (Miller et al., 2008). The manual bones follow isometry or negative allometry (becoming more slender), whilst the pedal bones tend to exhibit more positive allometry (Miller et al., 2008). Their study also showed that regions of the feet grow at different rates. The manual bones tend to grow fastest laterally (digits 4 and 5), whilst the pedal bones grow fastest medially (digit 1) and laterally (digits 4 and 5). Miller and colleagues attributed such growth differences to the variations in the mechanics that elephant feet experience during locomotion, and speculated that whilst regional pressure differences should increase with body mass, the highest pressures should occur on digits 4 and 5 in the manus and digits 1, 4 and 5 in the pes (Miller et al., 2008).
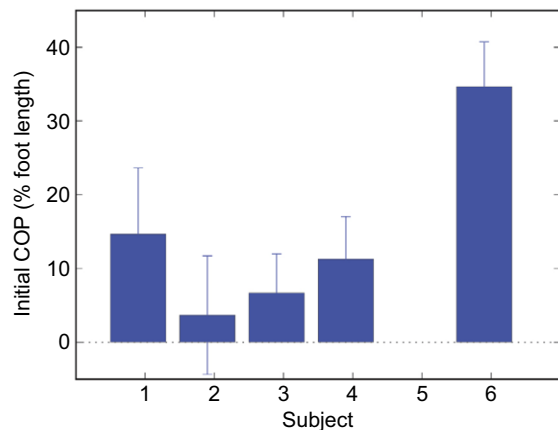
Fig. 10. COP trajectories resolved at initial foot contact into the percentage distance between the cranial- and caudal-most foot points.

Fig. 11. Example of an extreme case of osteoarthritis of digit 4 (right) of the elephant right manus against the non-pathological digit 4 of the left manus (left) of the same elephant.

The results of our study (hypothesis 1) only partially support Miller et al.'s proposal (Miller et al., 2008). Foot pressures increase across ontogeny (see below), but are not limited to a particular area of each foot, spanning broadly over most of each foot's sole surface. In particular, peak pressures are not increased for digit 1 in the pes as Miller et al. hypothesized (Miller et al., 2008), and are not limited to digits 4 and 5 for the manus and the pes. The highest pressures are encountered in digit 3 for both the manus and the pes. Peak pressures for digit 3 of the manus are approximately 8% higher than those for digits 4 and 5, whereas peak pressures for digits 4 and 5 are only 0.6% different (higher in digit 5 than 4). Differences between digits 3 and 4 are greatest for the pes, with digit 3 displaying peak pressure magnitudes that are higher than those for digits 4 and 5 by approximately 35% and 29%, respectively, at toe-off. Digit 5 of the pes displays pressure magnitudes 6% higher than those of digit 4.

Our results do not support hypothesis 2 (peak pressure in the manus and pes are maintained at a constant level with increasing size). Instead, we found that there is a positive correlation between body mass and peak pressures in our ontogenetic sample of elephants, showing that peak pressures adapt to size changes during growth and that elephants do not maintain the same spatiotemporal mechanics across ontogeny. This indicates that strict dynamic similarity is not maintained across ontogeny in elephant feet, even though it applies more generally to elephant kinematics across ontogeny (Hutchinson et al., 2006; Ren et al., 2008).

Our SPM results show significant inter-individual variability in whole-foot peak pressures between individuals of different body mass. The youngest elephant shows lower peak pressure values than the older elephants, which in turn increase their peak pressure values as they increase in body mass. Nevertheless, individuals of similar age and body mass did not display significant differences or variability in their peak pressure values across the whole foot. Intra-individual variation in peak pressures was encountered, but there was a general trend to develop the highest pressures laterally and in particular for digits 3, 4 and 5. Mean peak pressure magnitudes across the whole foot are generally higher for both right feet but only by about 10% and with evident intra-specific variation. In contrast, all subjects have significantly higher peak pressures for the manus than for the pes (by about 5%). Hence, the greater area and duty factor of the manus seem to compensate for the greater forces on the forelimbs (Hutchinson et al., 2006; Ren et al., 2010).

Our ROI results involve higher pressure values than the SPM results and exhibit a significant percentage difference (by about 73%) in peak regional pressure magnitudes between the manus and the pes. This difference in pressure magnitudes using the two different methods highlights the limitations of the estimation of foot pressure distribution over discrete zones alone because it does not take into consideration intra-zone variability, thus giving a biased high-pressure assessment of the overall foot pressure.

Our findings highlight the reduced pressures that characterize the caudal and central aspect (and, to a lesser degree, the medial aspect) of elephant feet during walking. Reduction of peak pressures must be partially caused by the highly compliant, fibrous fatty pad that dominates the foot area and associated structures such as the prepollex and prehallux ('predigits') which connect the proximal carpal/tarsal bones with the substrate and direct the GRF proximally rather than through the distal phalanges. It is thus curious that there is no clear concentration of pressures around the distal end of the predigits (caudal to ROI 1), but this could be explained by the spreading out of these pressures over the fat pad and sole. Regardless, the fat pad is highly viscoelastic and probably functions as a shock absorber (and pressure distributor) during locomotion.

Similar to the fat pad of the human heel, the elephant foot fat pad presumably functions as shock absorber when the foot hits the ground because of its viscoelastic properties. Thus, it is expected to reduce plantar/palmar pressures. Nevertheless, foot pressure reductions can also be achieved via increasing the surface area that the pressure is applied to, because pressure (P) equals force (F) per surface area (A). Our hypothesis 3 was not falsified, so perhaps reduction of pressure on the caudal and central aspect of the elephant foot fat pad is not solely due to its viscoelastic nature but results from a complex and dynamic interaction of behavioural preferences, as manifested in COP trajectories and viscoelastic material properties. This interaction may partly account for the ontogenetic reduction of the peak pressures of the manus relative to the pes.

Our results show that peak pressures which could cause damage to the soft tissue of the sole are mitigated both passively by the viscoelastic pad and behaviourally by temporal control of regional foot-loading patterns. COP trajectories in adults quickly shift from a slightly lateral position to a more central one following foot impact. They then display a craniocaudal pattern (excursion along the long axis of the foot) for most of the stance phase. Finally, the COP shifts cranio-medially during toe off, typically passing through the third digit (Fig. 9) – quite unlike humans (Lord, 1986) and bonobos (Vereecke et al., 2003). Both humans and bonobos direct forces more medially and through the digit that is located the most distally during toe off (digit 1 for humans; digits 1, 2 or 3 for bonobos).

Overall, the general COP trajectories of elephants are vaguely similar to the COP trajectories of humans and bonobos in being sigmoidal (passing from lateral to central, then medial), but with a much more mediolaterally compressed shape that is more linear than the typical human/primate pattern. Nonetheless, elephant COP trajectories share many similarities with those of another large mammal, the cow, which loads the lateral claw during impact, shifts the COP trajectories more medially during mid-stance and loads the middle cranial parts of the wall and the sole during toe-off (van der Tol et al., 2003). However, it is unclear how common this pattern is in other quadrupeds, especially large-bodied species (e.g. horses, giraffes, rhinoceroses), or how much diversity in other aspects of foot pressure patterns exists in such species.

COP trajectories in very young elephants are similar to those of the adults, but exhibit greater variability between and within individuals. Furthermore, as elephants grow larger, they shift the region of the foot impacting the ground cranially (away from the 'heel'). As a result, in larger, older elephants the foot is closer to horizontal at initial contact, showing that plantar and palmar contact pressures are distributed over a larger area during very early stance. The larger contact area may help achieve a more even distribution of plantar/palmar pressures and protect the caudal and central foot regions from excessive stresses and thus damage. These variable COP trajectory and roll-off patterns of very young individuals are presumably linked to their lack of experience in walking, similar to the plantar pressure profiles of human toddlers, which are initially highly variable and atypical of adults, but which rapidly mature thereafter (Bosch and Rosenbaum, 2010). We did not find other temporal changes in foot loading in our elephant subjects, but general ontogenetic changes of temporal parameters are predictable from previous kinematic studies – smaller elephants take quicker steps [shorter stance (i.e. contact) durations] but otherwise move similarly to adult elephants, and the manus stance durations (i.e. duty factors) remain slightly longer than for the pes (Hutchinson et al., 2006).

Digits 3–5 seem to be the areas of the most common occurrence of pathologies (e.g. Fig. 11) in elephants. The causes of foot pathologies in elephants are multifactorial (Csuti et al., 2001; Fowler and Mikota, 2006). Nevertheless, we find some support for the inference that there is a biomechanical link between regional peak pressures and the incidences of pathology in elephant feet (hypothesis 4). However, more rigorous statistical analyses of the distributions of pathologies in elephant feet are needed to test the largely anecdotal accounts that inspired our hypothesis. Contrary to the lateral aspect of the elephant feet, the medial, the central and the caudal aspects showed the lowest pressures and seem to have lower incidences of pathologies.

CONCLUSION

Using statistical parametric mapping we have presented the most complete study to date on the distribution and ontogenetic scaling of foot sole pressures in Asian elephants. We have shown that peak pressures adapt to size changes during growth and that elephant feet do not maintain the same spatiotemporal mechanics across ontogeny. We found significant variability between individuals with different body masses, but still uncovered a general trend for high lateral pressures, particularly in digits 3, 4 and 5. Our investigation of COP trajectories also revealed that peak pressures around the cranial and caudal aspects of the elephant feet are low, possibly due to the dynamic interaction of the viscoelastic fat pad coupled with

behavioural preferences by temporal control of regional foot-loading patterns. Finally, we discovered some support for the biomechanical link between regional peak pressures and the incidence of pathology in elephant feet as the highest pressures are encountered in digits 3–5, areas with the most common occurrence of pathologies based on anecdotal data from zoo keepers and our post-mortem database.

REFERENCES
Alexander, R. McN. and Jayes, A. S. (1983). A dynamic similarity hypothesis for the gaits of quadrupedal mammals. *J. Zool.* **201**, 135-152.
Alexander, R. McN., Bennet, M. B. and Ker, R. F. (1986). Mechanical properties and function of the paw pads of some mammals. *J. Zool.* **209**, 405-419.
Bosch, K. and Rosenbaum, D. (2010). Gait symmetry improves in childhood – a 4-year follow-up of foot loading data. *Gait Posture*, **32**, 464-468.
Csuti, B., Sargent, E. L. and Bechert, U. S. (2001). *The Elephant's Foot: Prevention and Care of Foot Conditions in Captive African and Asian Elephants.* Iowa: Iowa State University Press.
D'Août, K., Meert, L., Van Gheluwe, B., De Clercq, D. and Aerts, P. (2010). Experimentally generated footprints in sand: analysis and consequences for the interpretation of fossil and forensic footprints. *Am. J. Phys. Anthropol.* **141**, 515-525.
Fowler, M. E. and Mikota, S. K. (2006). Foot disorders. In *Biology, Medicine and Surgery of Elephants* (ed. M. E. Fowler and S. K. Mikota), pp. 271-290. Iowa: Blackwell Publishing.
Friston, K. J., Ashburner, J. T., Kiebel, S. J., Nichols, T. E. and Penny, W. D. (2007). *Statistical Parametric Mapping: The Analysis of Functional Brain Images.* London: Elsevier.
Hutchinson, J. R., Schwerda, D., Famini, D. J., Dale, R. H. I., Fisher, M. S. and Kram, R. (2006). The locomotor kinematics of Asian and African elephants: changes with speed and size. *J. Exp. Biol.* **209**, 3812-3827.
Lord, M., Reynolds, D. P. and Hughes, J. R. (1986). Foot pressure measurement: a review of clinical findings. *J. Biomed. Eng.* **8**, 283-294.
Maintz, J. B. A. and Viergever, M. A. (1998). A survey of medical image registration. *Med. Image Anal.* **2**, 1-37.
Michilsens, F., Aerts, P., Van Damme, R. and D'Août, K. (2009). Scaling of plantar pressures in mammals. *J. Zool.* **279**, 236-242.
Miller, C. E., Basu, C., Frisch, G. and Hutchinson, J. R. (2008). Ontogenetic scaling of foot musculoskeletal anatomy in elephants. *J. R. Soc. Interface* **5**, 465-475.
Oliveira, F. P. M., Pataky, T. C. and Manuel, J. (2010). Registration of pedobarographic image data in the frequency domain. *Comput. Methods Biomech. Biomed. Engin.* **13**, 731-740.
Pataky, T. C. (2008). Assessing the significance of pedobarographic signals using random field theory. *J. Biomech.* **41**, 2465-2473.
Pataky, T. C. and Goulermas, J. Y. (2008). Pedobarographic statistical parametric mapping (pSPM): a pixel-level approach to foot pressure image analysis. *J. Biomech.* **41**, 2136-2143.
Pataky, T. C., Caravaggi, P., Savage, R., Parker, D., Goulermas, J. Y., Sellers, W. I. and Crompton, R. H. (2008). New insights into the plantar pressure correlates of walking speed using pedobarographic statistical parametric mapping (pSPM). *J. Biomech.* **41**, 1987-1994.
Ren, L., Butler, M., Miller, C., Schwerda, D., Fischer, M. and Hutchinson, J. R. (2008). The movements of limb segments and joints during locomotion in African and Asian elephants. *J. Exp. Biol.* **211**, 2735-2751.
Ren, L., Miller, C. E., Lair, R. and Hutchinson, J. R. (2010). Integration of biomechanical compliance, leverage, and power in elephant limbs. *Proc. Natl. Acad. Sci. USA* **117**, 7078-7082.
van der Tol, P. P. J., Metz, J. H. M., Noordhuizen-Stassen, E. N., Back, W., Braam, C. R. and Weijs, W. A. (2003). The vertical ground reaction force and the pressure distribution on the claws of dairy cows while walking on a flat substrate. *J. Dairy Sci.* **86**, 2875-2883.
Vereecke, E. E., D'Août, K., De Clercq, D., Van Elsacker, L. and Aerts, P. (2003). Dynamic plantar pressure distribution during terrestrial locomotion of bonobos (*Pan paniscus*). *Am. J. Phys. Anthropol.* **120**, 373-383.
Weissengruber, G. E., Egger, G. F., Hutchinson, J. R., Groenewald, H. B., Elsasser, L., Famini, D. and Forstenpointner, G. (2006). The structure of the cushions in the feet of African elephants (*Loxodonta africana*). *J. Anat.* **209**, 781-792.